Available online at www.sciencedirect.com
SCIENCE DIRECT
Journal of Sound and Vibration 294 (2006) 547–561
JOURNAL OF SOUND AND VIBRATION
www.elsevier.com/locate/jsvi

Dynamic modelling of spur gear pair and application of empirical mode decomposition-based statistical analysis for early detection of localized tooth defect

A. Parey[a], M. El Badaoui[b], F. Guillet[b], N. Tandon[a,*]

[a]*Industrial Tribology, Machine Dynamics and Maintenance Engineering Centre, Indian Institute of Technology Delhi, Hauz Khas, New Delhi-110016, India*
[b]*Laboratoire d'Aalyse des Signaux & des Processus Industriels, IUT de Roanne, 20, Avenue de Paris, 42 334 Roanne, France*

Received 15 September 2004; received in revised form 30 August 2005; accepted 26 November 2005
Available online 23 March 2006

Abstract

Gears are one of the most common and important machine components in many advanced machines. An improved understanding of vibration signal is required for the early detection of incipient gear failure to achieve high reliability. This paper mainly consists of two parts: in the first part, a 6-degree-of-freedom gear dynamic model including localized tooth defect has been developed. The model consists of a spur gear pair, two shafts, two inertias representing load and prime mover and bearings. The model incorporates the effects of time-varying mesh stiffness and damping, backlash, excitation due to gear errors and profile modifications. The second part consists of signal processing of simulated and experimental signals. Empirical mode decomposition (EMD) is a method of breaking down a signal without leaving a time domain. The process is useful for analysing non-stationary and nonlinear signals. EMD decomposes a signal into some individual, nearly monocomponent signals, named as intrinsic mode function (IMF). Crest factor and kurtosis have been calculated of these IMFs. EMD pre-processed kurtosis and crest factor give early detection of pitting as compared to raw signal.

1. Introduction

Dynamic modelling of the gear vibration is a useful tool to study the vibration response of a geared system under various gear parameters and operating conditions. A comprehensive review of mathematical models used in gear dynamics, published before 1986, has been presented by Ozguven and Houser [1]. In this review, gear dynamic models without defects have been discussed. In the past few years, researchers have been working on the gear dynamic models which include defects like pitting, spalling, crack and broken tooth.

*Corresponding author. Tel.: +91 11 26591276; fax: +91 11 26596222.
E-mail address: ntandon@itmmec.iitd.ernet.in (N. Tandon).

0022-460X/$ - see front matter © 2006 Elsevier Ltd. All rights reserved.
doi:10.1016/j.jsv.2005.11.021

Nomenclature

c_1, c_2	viscous damping coefficients of pinion and gear bearings, respectively
c_a, c_b	viscous damping coefficients of the first and second meshing tooth pairs, respectively
c_m	mesh damping
c_{t1}, c_{t2}	viscous damping coefficients of pinion and gear shafts, respectively
I_D, I_1, I_2, I_L	mass moment of inertia of drive, pinion, gear and load, respectively
k_1, k_2	pinion and gear bearing stiffness, respectively
k_a, k_b	the single tooth pair stiffness at contact points A and B
k_h	the unit width Hertzian stiffness
k_m	time-varying mesh stiffness
k_{t1}, k_{t2}	torsional stiffness of pinion and gear shafts, respectively
m_1, m_2	masses of pinion and gear, respectively
R_1, R_2	base circle radii of pinion and gear, respectively
T_D, T_L	drive and load torques, respectively
y_1, y_2	translational displacement of pinion and gear, respectively
θ_D, θ_1, θ_2, θ_L	angular displacement of drive, pinion, gear and load

A review of spur gear dynamic models including defects has been done by Parey and Tandon [2]. The study suggests that little work has been done on modelling of gear vibration with defect and an accurate analytical procedure to predict gear vibrations in the presence of local tooth fault has yet to be developed.

A wide variety of dynamic models, from single degree of freedom to multi degrees of freedom, are available to predict the response of gear vibration. To increase the accuracy of the dynamic model for prediction of vibration response, researchers either increase the degrees of freedom from single to multi degrees, or include various effects like nonlinearity of the elements, excitation due to gear errors, time variation of mesh stiffness, etc. in the model, or both. The purpose of the dynamic simulation plays a very important role in constructing a suitable model. The purpose of this paper is to develop a multi-degree-of-freedom nonlinear model for a spur gear pair that can be used to study the effect of lateral–torsional vibration coupling on vibration response in the presence of localized tooth defect. A typical fault signal is assumed to be impulsive in nature because of the way it is generated [3]. The surface defects on gear tooth will produce pressure fluctuations in the lubricant and the oil film between sliding surfaces may also momentarily break down, causing impulsive contact to occur. In an earlier work by Tandon and Choudhary, an analytical model for the prediction of the vibration response of rolling element bearing due to localized defect has been developed using impulse phenomenon [4]. The effect of changes in magnitude and phase of the mesh stiffness has been used by the researchers to simulate the effects of surface pitting and wear [5–7]. But no work has been reported using the impulse phenomenon to simulate the pitting in gear pair. In this paper, a decaying sinusoidal pulse has been used to simulate the effect of pitting in the gear dynamic model.

A wide variety of signal-processing techniques are available for gear fault detection. These techniques can be classified as signal processing based on time domain signal [7–12], frequency domain signal [13–15] and time–frequency domain signal [16–20]. Each technique has some advantages and some limitations over the other.

Recently, empirical mode decomposition (EMD) has been introduced for the analysis of nonlinear and non-stationary signals [21]. EMD is a time-adaptive decomposition operation of the signal, which decomposes the signal into a set of complete, and almost orthogonal components, named as intrinsic mode function (IMF). IMFs are almost mono components and represent simple oscillatory modes imbedded in the signal. Crest factor and kurtosis have been performed on different IMFs for early detection of the pitting. Crest factor and kurtosis are statistical parameters that give a measure of the impulsiveness of a signal, and therefore they are well suited for the developed model.

2. Generation of the mathematical model

In most of the gear pair systems, the coupling between the torsional vibration modes is controlled by mesh stiffness; therefore a 2-degree-of-freedom semi-definite mathematical model representing only the torsional

vibration may yield a quite accurate result in most practical cases. [22]. When the torsional mode which is controlled by mesh stiffness is coupled with other vibration modes, in such problems, increasing the degrees of freedom of the model by including the compliances of other element is more important than elaborating the single-degree-of-freedom model with some secondary effects. The model described in this paper is based on the model developed by Ozguven [23]. This model is modified by excluding some effect for simplicity, and including impulse excitation generated due to localized tooth defect.

2.1. Six-degree-of-freedom nonlinear model

The model considered here consists of two gears on the two shafts, which are connected to a load and a prime mover. The model includes four inertias, namely load, prime mover, pinion and gear. The torsional compliances of shafts and the transverse compliances of bearings combined with those of shafts are included in the model. Both bearing and shaft dampings are also considered in the model. The transverse vibrations of the gears are considered along the line of action. With this model, the response, including modulations due to transverse and torsional vibration stemming from bearing and shaft compliances, can be calculated.

The 6-degree-of-freedom nonlinear model is shown in Fig. 1. It has four angular rotations (of prime mover, pinion, gear and load) and two translations (of pinion and gear) along the line of action. The effects that are included in the mathematical model and thus considered in the dynamic analysis are: time-varying mesh stiffness and mesh damping; torsional compliances of pinion and gear shafts; material damping in shafts (linear viscous); bearing compliances and dampings (linear viscous); transverse compliances of shafts; inertia of prime mover and load; drive and load torques and backlash.

The governing equations of motion for the model depicted in Fig. 1 can be written as follows (a list of symbols is given in the Nomenclature):

$$I_D\theta''_D + c_{t1}(\theta'_D - \theta'_1) + k_{t1}(\theta_D - \theta_1) = T_D, \tag{1}$$

$$I_1\theta''_1 + c_{t1}(\theta'_1 - \theta'_D) + k_{t1}(\theta_1 - \theta_D) = -W_0R_1, \tag{2}$$

$$I_2\theta''_2 + c_{t2}(\theta'_2 - \theta'_L) + k_{t2}(\theta_2 - \theta_L) = W_0R_2, \tag{3}$$

$$I_L\theta''_L + c_{t2}(\theta'_L - \theta'_2) + k_{t2}(\theta_L - \theta_2) = -T_L, \tag{4}$$

$$m_1y''_1 + c_1y'_1 + k_1y_1 = W_0, \tag{5}$$

$$m_2y''_2 + c_2y'_2 + k_2y_2 = -W_0. \tag{6}$$

Here, W_0 is the dynamic mesh force given by

$$W_0 = k_m(\theta_1R_1 - \theta_2R_2 + y_2 - y_1) + c_m(\theta'_1R_1 - \theta'_2R_2 + y'_2 - y'_1) \tag{7}$$

and $'$ denotes differentiation with respect to time.

2.2. Incorporation of profile error

Since every gear has some deviation from the actual involute profile, it has to be taken into account. For a given pair of teeth, the value of an error is random and it can be denoted by [24]

$$E_n = [1 - r(1 - l_i)]e, \tag{8}$$

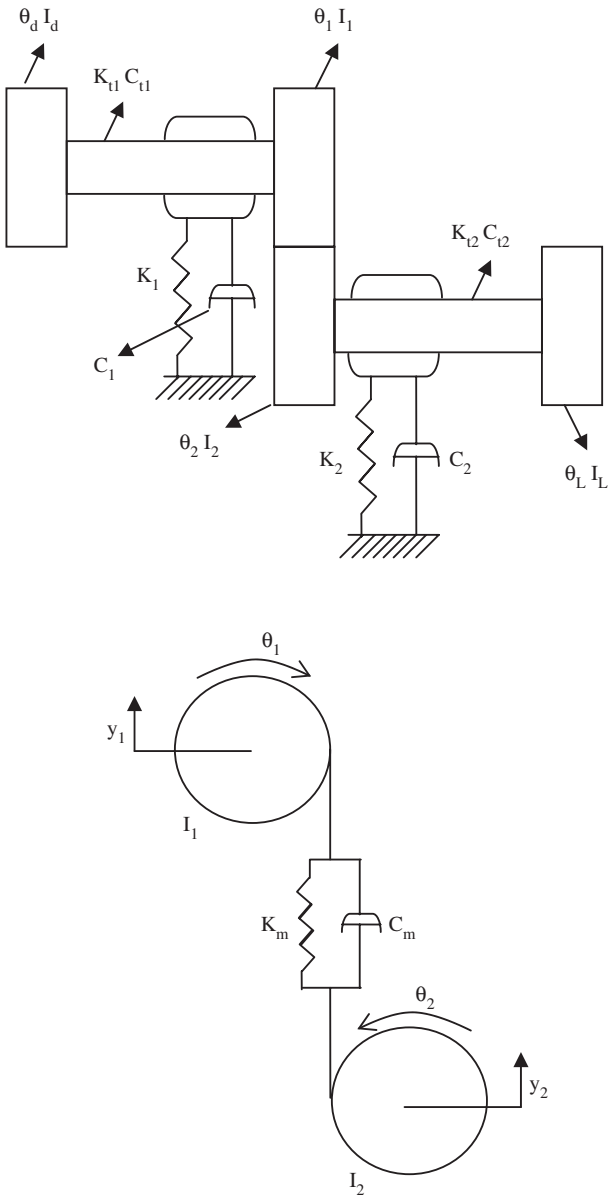

Fig. 1. The 6-degree-of-freedom nonlinear model.

where e is the maximum error value; r is the coefficient of error variation, range (0–1); and l_i is a random value whose elements are normally distributed with mean 0, variance 1 and standard deviation 1 and range (0–1); n is the number of teeth pair.

2.3. Incorporation of eccentricities

The influence of eccentricities can be investigated by incorporating it in the error function. The eccentricities can be modelled as [24]

$$E = e_1 \sin(\theta_1) + e_2 \sin(\theta_2), \tag{9}$$

where e_1 is the eccentricity of gear 1 and e_2 the eccentricity of gear 2.

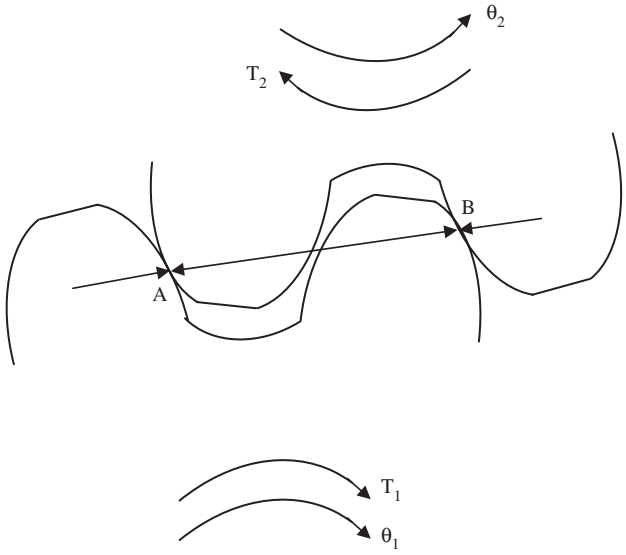

Fig. 2. Response of a decaying half-sine pulse train.

2.4. Incorporation of defect

It has been pointed out in Ref. [3] that the severity, extent and age of damage can be better represented by pulses. The height of the pulse also has a significant influence on the amplitude. This also changes with the severity and age of the defect and may even decrease with the advancement of the defect [3]. Rectangular pulses could be considered as the simplest impulsive loading, but in practice the shape of the signal will be controlled by the nature of the system in addition to the type of exciting force. In a gear pair system due to the deformation and elasticity of the contacting components, neither the force nor the response time history will have the shape of rectangular pulses. To model the signal more representatively, half-sine pulses are considered. The response of the practical system can be best represented by decaying sinusoid as shown in Fig. 2, given by

$$x(t) = \left(K/\sqrt{1-\zeta^2}\right) e^{-\zeta\omega_0 t} \sin\left\{\sqrt{1-\zeta^2}\omega_0 t + \sin^{-1}\left(2\zeta\sqrt{1-\zeta^2}\right)\right\}, \tag{10}$$

where $K = k/\sqrt{1-\zeta^2}$ and k is the height of the pulse; ζ is the damping ratio; frequency of generated pulse $\omega_0 = \pi/\Delta t$; pulse width $\Delta t = b/v_a$; b is the defect width in profile direction and v_a is the relative velocity at the defect point.

After including the profile error, eccentricities and defect, the dynamic mesh force W_0 can be modified as

$$W = W_0 + k_a(E_1 + E) + k_b(E_2 + E) + c_1(E_1 + E) + c_2(E_2 + E) + k_h(x(t))f, \tag{11}$$

where f is the defect width in face direction.

So, by putting Eq. (11) in Eqs. (2), (3), (5) and (6) in place of W_0 and solving the differential equations, we can find the response of the system at the desired place.

2.5. Solution

To solve the differential equations (1)–(6), each second-order differential equation is written in the form of two first-order differential equations. Thus, 12 nonlinear first-order differential equations were obtained. These equations were written such that each equation contains the time derivative of only one variable. These equations were solved by MATLAB code equation solvers.

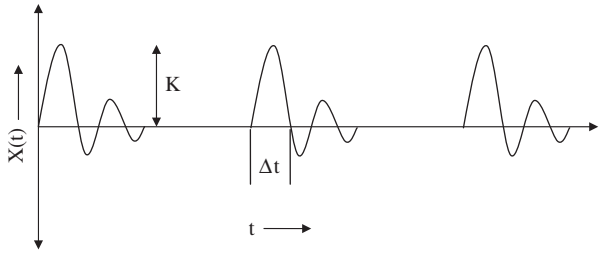

Fig. 3. Two teeth pairs of a spur gear in contact.

2.6. Calculation of mesh stiffness

The mesh stiffness between an engaged gear pair consists of two parts: one associated with the local Hertzian deformation and the other associated with the tooth bending deflection. The unit width Hertzian stiffness k_h resulting from the tooth surface contact was first approximated by Yang [25] as

$$k_h = \pi E/4(1-v^2), \tag{12}$$

where E is Young's modulus and v is the Poisson's ratio.

An equation for the calculation of single tooth bending stiffness for the addendum-modified involute gear has been proposed by Kuang and Yang [26]. The unit width stiffness $k_i(r)$ for a single tooth i at a loading position r can be approximated using the following equation:

$$k_i(r) = (A_0 + A_1 X_i) + (A_2 + A_3 X_i)[(r - R_i)/(1 + X_i)m], \tag{13}$$

where the bending stiffness per unit tooth width $k_i(r)$ is measured in N/μm/mm .Variable X_i denotes the addendum modification coefficient. The radial distance r, radius of pitch circle R and the module m are measured in the same unit (mm). The curve-fitted coefficients are:

$$\begin{aligned} A_0 &= 3.867 + 1.612N_i - 0.02916N_i^2 + 0.0001553N_i^3, \\ A_1 &= 17.06 + 0.7289N_i - 0.01728N_i^2 + 0.0000999N_i^3, \\ A_2 &= 2.637 - 1.222N_i + 0.02217N_i^2 - 0.0001179N_i^3, \\ A_3 &= -6.330 - 1.033N_i + 0.02068N_i^2 - 0.0001130N_i^3, \end{aligned} \tag{14}$$

where N_i is the number of teeth.

The single tooth pair stiffness k_a and k_b at contact points A and B, as shown in Fig. 3, can be approximated by combining the unit width stiffness $k_1(r_{1A})$, $k_2(r_{2A})$, $k_1(r_{1B})$, $k_2(r_{2B})$ and k_h of mating teeth as spring connected in series:

$$1/ka = 1/k_1(r_{1A}) + 1/k_2(r_{2A}) + 1/k_h, \tag{15}$$

$$k_a/F = [k_1(r_{1A})k_2(r_{2B})k_h]/[k_1(r_{1A})k_2(r_{2A}) + k_1(r_{1A})k_h + k_2(r_{2A})k_h], \tag{16}$$

$$1/k_b = 1/k_1(r_{2B}) + 1/k_2(r_{2B}) + 1/k_h, \tag{17}$$

$$k_b/F = [k_1(r_{1B})k_2(r_{2B})k_h]/[k_1(r_{1B})k_2(r_{2A}) + k_1(r_{1A})k_h + k_2(r_{2A})k_h], \tag{18}$$

where k_a and k_b represent the single tooth pair stiffness of gears 1 and 2 at mating points A and B. They are measured in (N/mm). F denotes the tooth width of a spur gear. In this system, the mesh stiffness of engaged gear pair alternates with the change of contact position and the number of load-sharing tooth pairs.

3. Signal-processing technique

As mentioned in Section 1, among various signal-processing techniques crest factor and kurtosis analysis have been used for analysing EMD pre-processed signal for the early detection of fault. In this section, crest factor, kurtosis and EMD have been explained.

3.1. Crest factor

The crest factor corresponds to the ratio between the crest value (maximum absolute value reached by the function representative of the signal during the considered period of time) and the root mean square (rms) value (efficient value) of the signal:

$$\text{Crest factor} = \textit{Crest value}/\textit{rms value} = \frac{\sup|x(n)|}{\sqrt{(1/N)\sum_{n=1}^{N}[x(n)]^2}}, \tag{19}$$

where N is the number of samples taken within the signal and $x(n)$ the time domain signal.

3.2. Kurtosis

It is a statistical analysis of the time domain signal, and looks at the fourth moment of the spectral amplitude difference from the mean level.

Mathematically,

$$K = 1/\sigma^4 \sum_{i=1}^{N}(x_i - x')^4/N, \tag{20}$$

where σ^4 is the variance square, N is the number of samples, x' is the mean value of samples and x_i is an individual sample. A normal distribution has a kurtosis value of 3 and it shows the good condition.

3.3. Empirical mode decomposition (EMD)

The EMD method is developed from the simple assumption that any signal consists of different simple intrinsic modes of oscillations. Each linear or nonlinear mode will have the same number of extrema and zero-crossings. There is only one extremum between successive zero-crossings. Each mode should be independent of the others. In this way, each signal could be decomposed into a number of IMFs, each of which must satisfy the following conditions [21]:

(1) In the whole data set, the number of extrema and the number of zero-crossings must either equal or differ at most by one.
(2) At any point, the mean value of the envelope defined by local maxima and the envelope defined by the local minima is zero.

An IMF represents a simple oscillatory mode compared with the simple harmonic function.

With the definition of EMD, any signal $x(t)$ can be decomposed as follows [21]:

Firstly identify all the local extrema, and then connect all the local maxima by a cubic spline line as the upper envelope. Repeat the procedure for the local minima to produce the lower envelope. The upper and lower envelopes should cover all the data between them. The mean of upper and lower envelope values is designated as m_1, and the difference between the signal $x(t)$ and m_1 is the first component, h_1; i.e.

$$x(t) - m_1 = h_1. \tag{21}$$

Ideally, if h_1 is an IMF, then h_1 is the first component of $x(t)$.

If h_1 is not an IMF, h_1 is treated as the original signal and the above procedure is repeated; then

$$h_1 - m_{11} = h_{11}. \tag{22}$$

After repeated sifting, i.e. up to k times, h_{1k} becomes an IMF, that is

$$h_{1(k-1)} - m_{1k} = h_{1k}. \tag{23}$$

Then it is designated as

$$c_1 = h_{1k}. \tag{24}$$

The first IMF component is obtained from the original data. c_1 should contain the finest scale or the shortest period component of the signal.

Separating c_1 from $x(t)$, We get

$$r_1 = x(t) - c_1, \tag{25}$$

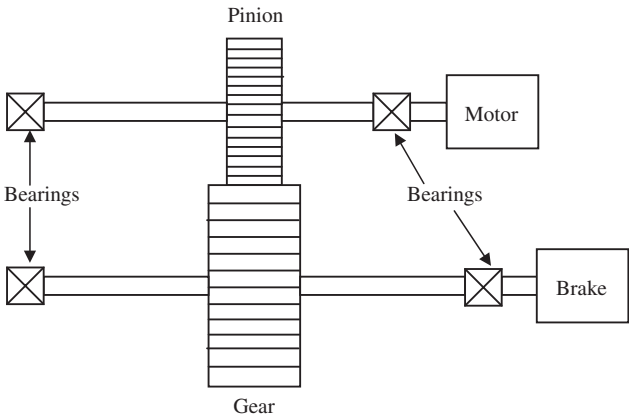

Fig. 4. Schematic representation of the geared system.

Table 1
Geared system data

Parameter	Pinion	Gear
Speed (rpm)	1000	952
Number of teeth	20	21
Face width (m)	0.015	0.03
Shaft diameter (m)	0.092	0.110
Module (m)	0.01	0.01
Pressure angle	20°	20°
Addendum coefficient	1.0	1.0
Dedendum coefficient	1.4	1.4
Mass (N)	36	80
Shaft torsional stiffness (N m/rad)	1917	3383
Bearing stiffness (N/m)	10^8	10^9
Shaft viscous damping coefficient (N s/rad)	0.268881	0.357188
Bearing viscous damping coefficient (N s/m)	8740.15	8740.15
Drive torque (N m)	200	

Table 2
Simulated defect

Defect number	Width in profile direction (mm)	Length in face direction (mm)	Location of defect
0	No defect		
1	1	0.25	Near pitch line
2	1	0.5	Near pitch line
3	1	0.75	Near pitch line
4	1	1.0	Near pitch line
5	1	1.25	Near pitch line
6	1	1.5	Near pitch line
7	1	1.75	Near pitch line
8	1	2.0	Near pitch line
9	1	2.25	Near pitch line
10	1	2.5	Near pitch line

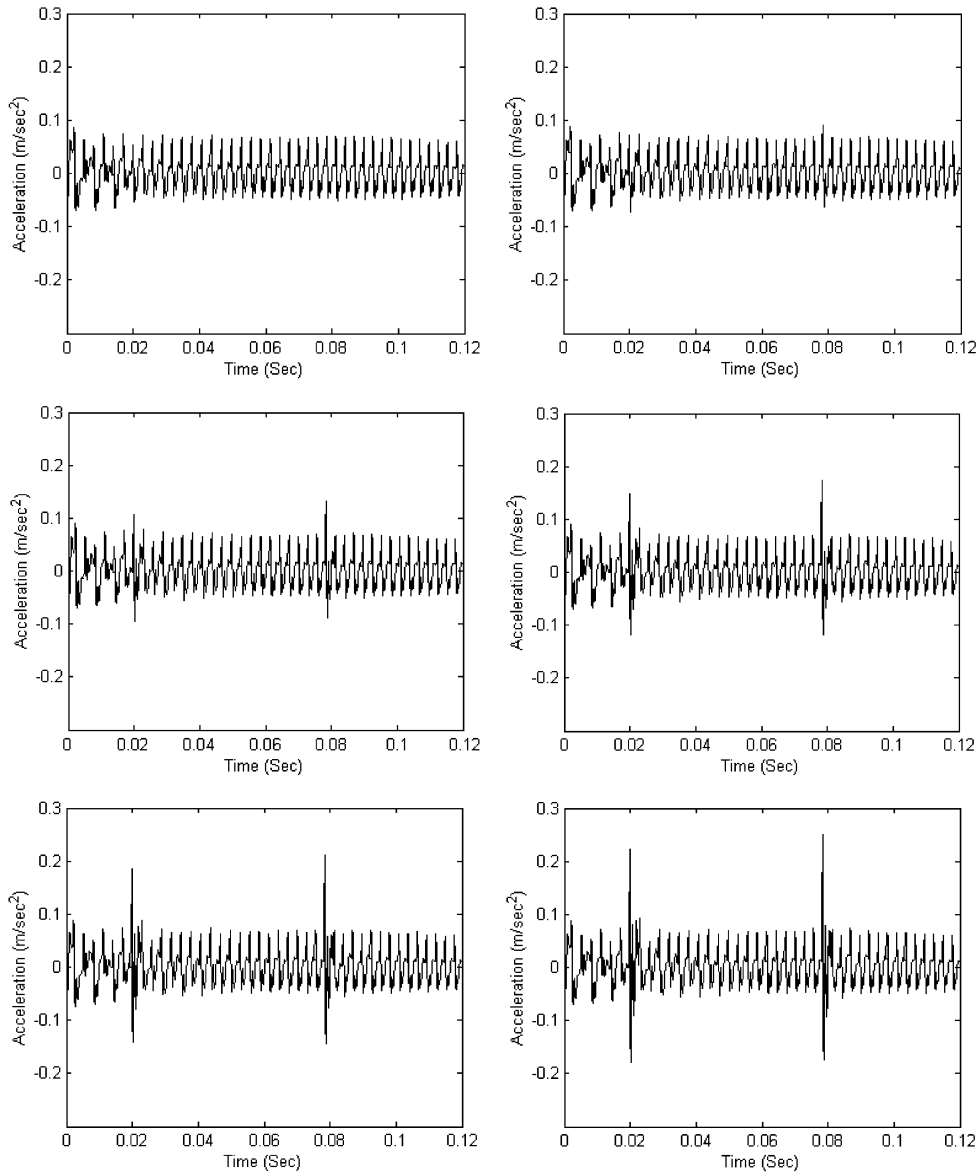

Fig. 5. Simulated acceleration for different defect length.

where r_1 is treated as the original data and the above process is repeated. The second IMF component c_2 of $x(t)$ could be obtained. If the process as described above is repeated n times, then n-IMFs of signal $x(t)$ can be obtained. Then,

$$\begin{aligned} r_1 - c_2 &= r_2 \\ &\vdots \\ &\vdots \\ r_{n-1} - c_n &= r_n. \end{aligned} \tag{26}$$

The decomposition process can be stopped when r_n becomes a monotonic function, from which no more IMFs can be extracted. By summing up Eqs. (25) and (26),

$$x(t) = \sum_{j=1}^{n} c_j + r_n. \tag{27}$$

Thus, one can achieve a decomposition of the signal into n-empirical modes and a residue r_n, which is the mean trend of $x(t)$. The IMFs $c_1, c_2, \ldots, c_n$ include different frequency bands ranging from high to low. The frequency components contained in each frequency band are different and they change with the variation of signal $x(t)$, while r_n represents the central tendency of signal $x(t)$.

4. Implementation of EMD

4.1. Numerical examples

The mechanical system under consideration is shown in Fig. 4. The different dynamic and design parameters of the gear system are given in Table 1. The mathematical model developed in Section 2 is solved using gear parameters given in Table 1. The model is solved for different defect conditions as given in Table 2. Some simulated results for two revolutions of the pinion are shown in Fig. 5. Crest factor and kurtosis value have been calculated for all the simulated defect width. Fig. 6 shows the plot for these values. The signal is

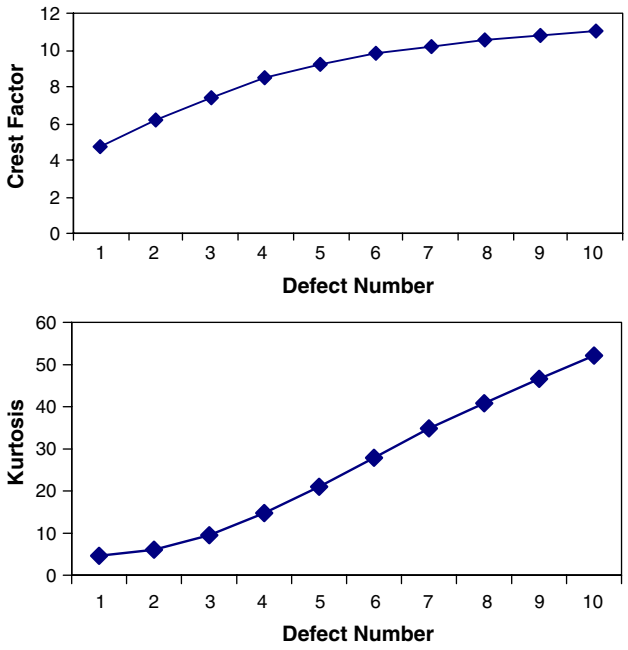

Fig. 6. Crest factor and kurtosis values of simulated acceleration.

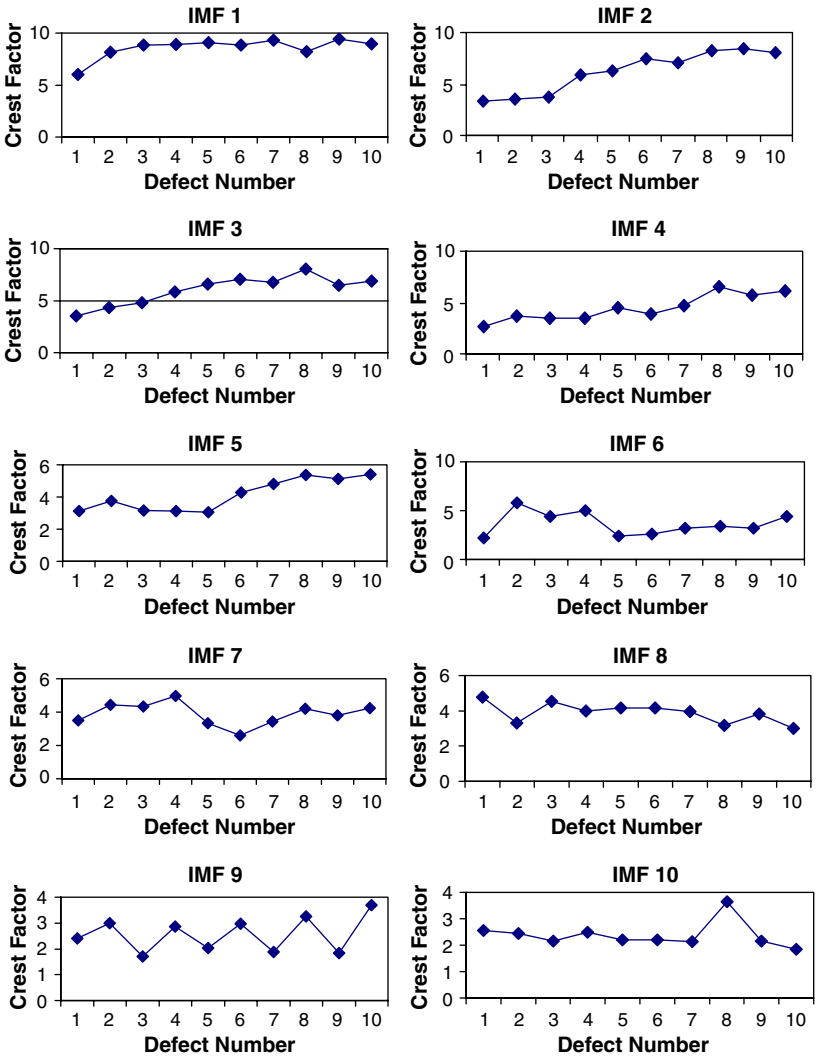

Fig. 7. Crest factor values of IMFs of the simulated signal.

decomposed by the EMD method as described in Section 3.3. The first 10 IMFs were calculated. Crest factor and kurtosis values have been calculated of these IMFs. Fig. 7 shows the crest factor values and Fig. 8 shows the kurtosis values for different simulated defect widths of each IMF.

4.2. Experimental example

The recordings of vibration signal were carried out at CETIM, France on a gear system with a train of gearing, with a ratio of 20/21 functioning continuously until its destruction. Table 1 gives the details of the gear test rig parameters. The test was of 13 days length with a daily mechanical appraisal; measurements were collected every 24 h. A fault was found on day 10. The acceleration signals for days 2, 10, 11, and 12 have been shown in Fig. 9. The kurtosis values for the experimental signal were calculated from day 2 to 13 and are shown in Fig. 10 (on day 1 no signal was taken). The signal is decomposed by the EMD method as described

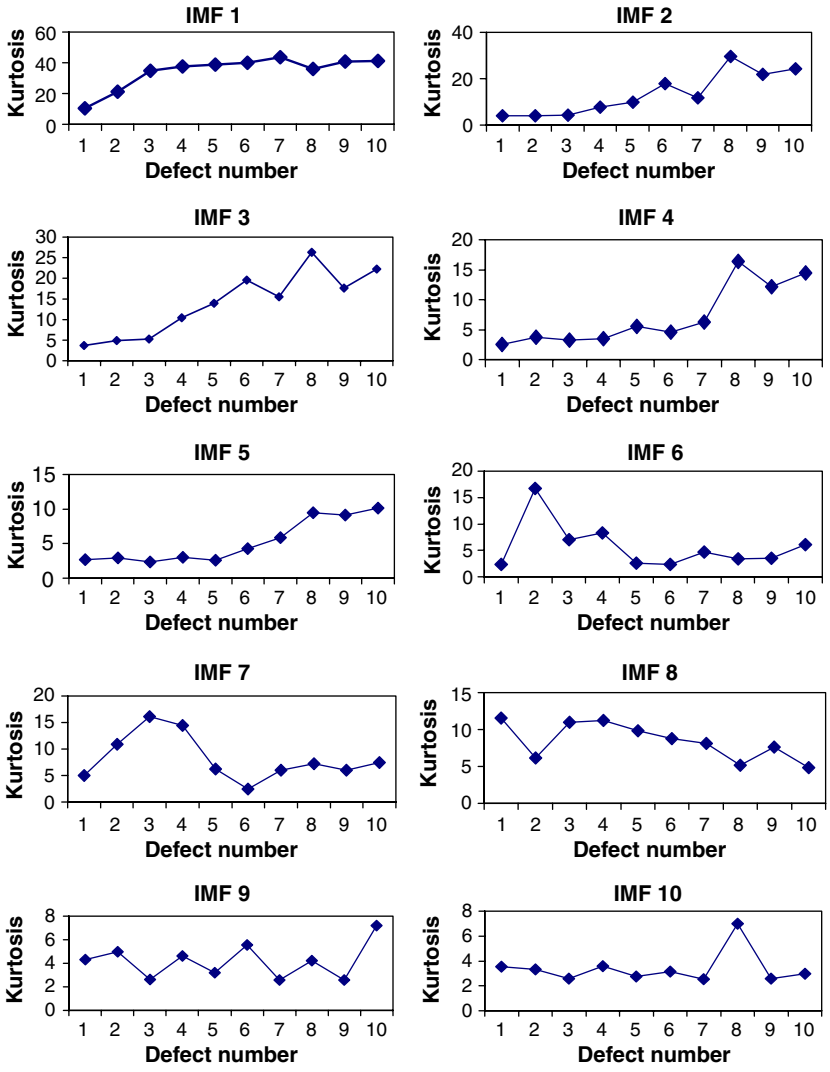

Fig. 8. Kurtosis values of IMFs of the simulated signal.

in Section 3.3. The first 10 IMFs were found. Kurtosis values have been calculated of these IMFs and are shown in Fig. 11.

5. Discussion and conclusion

The simulated signal shows that as the defect size increases the amplitude of the acceleration signal increases. The experimental signal also shows the similar results. The crest factor and kurtosis values of the simulated signal increase as the fault increases. The crest factor and kurtosis values of IMFs of the simulated signal suggest that the crest factor and kurtosis values of high-frequency IMF (harmonics of gear mesh frequency, IMF 1–5) increase as the fault increases. The crest factor and kurtosis values of middle-frequency IMF (gear mesh frequency and below, IMF 5–7) first increase and than decrease. The crest factor and kurtosis values of low-frequency IMF (gear rotational frequency and lower harmonics, IMF 8–10) almost remain constant. Though the crest factor and kurtosis values give similar trends, kurtosis is a better indicator as

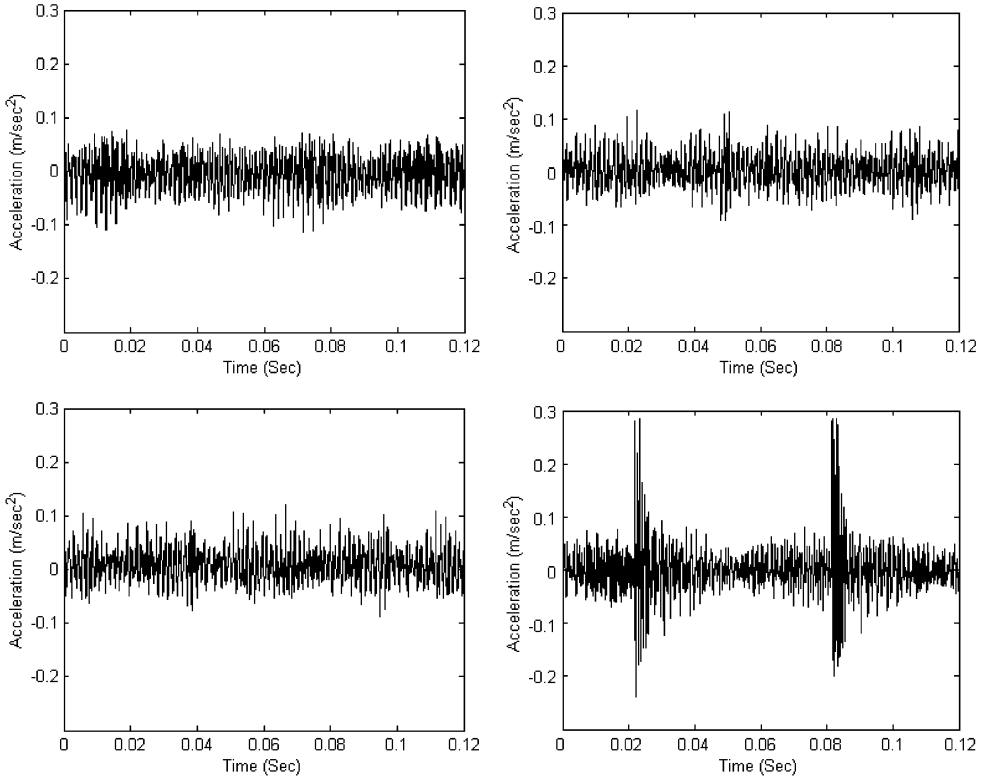

Fig. 9. Experimental acceleration signal for days 2, 10–12.

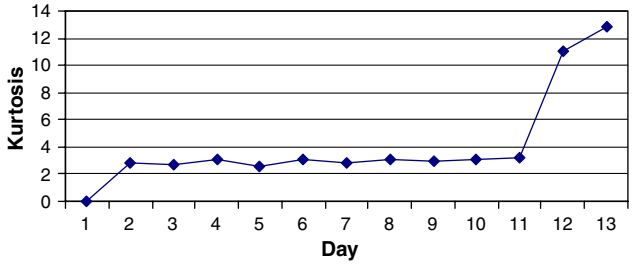

Fig. 10. Kurtosis value of the experimental signal from day 2 to 13.

compared to crest factor. To analyse the experimental signal, only kurtosis value has been discussed. The kurtosis value of raw experimental signal (without EMD) increases rapidly after day 11, which indicates development of the fault. But, when the signal is decomposed by EMD and kurtosis value is calculated of each IMF, fault can be detected on day 10, as the kurtosis value starts increasing from day 10 in the high-frequency range.

Although experimental and numerical results look promising, the proposed vibration signature methodology has to be tested on the other test rig also. More work is also required on the simulation of tooth faults by varying defect width in both directions. Kurtosis analysis of IMF could be a good indicator for early detection and characterization of faults.

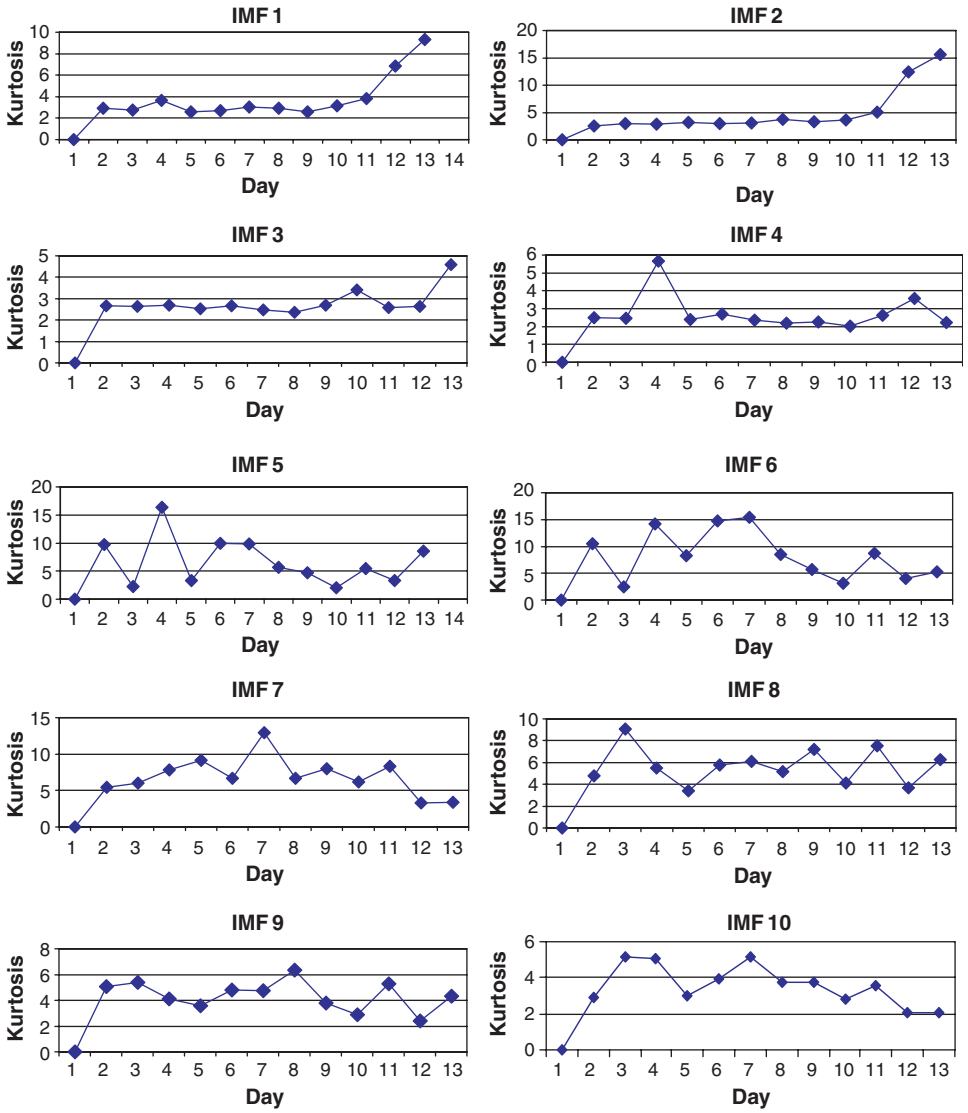

Fig. 11. Kurtosis values of IMFs of experimental signal.

Acknowledgments

The authors gratefully acknowledge the support of CETIM and G.D.R. - P.R.C. ISIS Unite G-720, which provided the experimental results.

References

[1] H.N. Ozguven, D.R. Houser, Mathematical models used in gear dynamics—a review, *Journal of Sound and Vibration* 121 (1988) 383–411.
[2] A. Parey, N. Tandon, Spur gear dynamic models including defects—a review, *The Shock and Vibration Digest* 35 (6) (2003) 465–478.
[3] M.F. White, Simulation and analysis of machinery fault signals, *Journal of Sound and Vibration* 93 (1) (1984) 95–116.

[4] N. Tandon, A. Choudhury, An analytical model for the prediction of the vibration response of rolling element bearing due to a localized defect, *Journal of Sound and Vibration* 205 (3) (1997) 275–292.
[5] F.K. Choy, V. Polyschuk, J.J. Zakrajsek, R.F. Handschuh, D.P. Townsend, Analysis of the effects of surface pitting and wear on the vibration of a gear transmission system, *Tribology International* 29 (1) (1996) 77–83.
[6] S.P. Yao, P.D. McFadden, Study of modelling for monitoring of gearbox vibration, *Third International Conference on Acoustical and Vibratory Surveillance Methods and Diagnostic Techniques*, Senlis, France, October 1998, pp. 555–564.
[7] M. El. Badaoui, V. Cahouet, F. Guillet, J. Danière, P. Velex, Modelling and detection of localized tooth defects in geared systems, *Transcations of the ASME* 123 (2001) 422–430.
[8] P.D. McFadden, J.D. Smith, A signal processing technique for detecting local defects in a gear from the signal average of the vibration, *Proceedings of the Institution of Mechanical Engineers* 199 (C4) (1985) 287–292.
[9] P.D. McFadden, Detecting fatigue cracks in gear by amplitude and phase demodulation of the meshing vibration, *ASME Transactions, Journal of Vibration, Acoustics, Stress and Reliability in Design* 108 (1986) 165–170.
[10] P.D. McFadden, Examination of a technique for the early detection of failure in gears by signal processing of the time domain average of the meshing vibration, *Mechanical Systems and Signal Processing* 1 (2) (1987) 173–183.
[11] R.B. Randall, Cepstral analysis and gearbox fault diagnosis, *Bruel and Kjaer Technical Bulletin*, second ed., 1980, pp. 1–19.
[12] M.El. Badaoui, J. Antoni, F. Guillet, J. Danière, P. Velex, Use of the moving cepstrum integral to detect and localise tooth spalls in gears, *Mechanical Systems and Signal Processing* 15 (5) (2001) 873–885.
[13] K. Fujita, A. Yoshida, K. Ota, On the possibility of early detection of gear tooth failures by noise and vibration, *Proceedings of the Sixth World Congress on Theory of Machine and Mechanisms* (1983) 668–672.
[14] P.D. McFadden, J.D. Smith, A signal processing technique for detecting local defects in gears from the signal average of the vibration, *Proceedings of the Institute of Mechanical Engineers* 199 (C4) (1985) 287–292.
[15] P.D. McFadden, Low frequency vibration measurement generated by gear teeth impacts, *NDT International* 18 (5) (1985) 279–282.
[16] B.D. Forrester, Analysis of gear vibration in the time-frequency domain, *Proceedings of the 44th Meeting of the Mechanical Failures Prevention Group of the Vibration Institute*, Virginia Beach, VA, 1990, pp. 225–234.
[17] W.J. Wang, P.D. McFadden, Early detection of gear failure by vibration analysis—part I. Calculation of the time–frequency distribution, *Mechanical Systems and Signal Processing* 7 (3) (1993) 193–203.
[18] S.T. Lin, P.D. McFadden, Vibration analyses of gearboxes by the linear wavelet transform, *Proceedings of the Institute of Mechanical Engineers* C492/007/95 (1995) 59–72.
[19] W.J. Wang, P.D. McFadden, Application of wavelet to gearbox vibration signal for fault detection, *Journal of Sound and Vibration* 192 (5) (1996) 927–939.
[20] W.J. Staszeski, G.R. Tomlinson, Applications of the wavelet transform to fault detection in a spur gear, *Mechanical Systems and Signal Processing* 8 (3) (1994) 289–307.
[21] N.E. Huang, Z. Shen, S.R. Long, M.L.C. Wu, H.H. Shih, Q.N. Zheng, N.C. Yen, C.C. Tung, H.H. Liu, The empirical mode decomposition and the Hilbert spectrum for nonlinear and non-stationary time series analysis, *Proceedings of the Royal Society of London Series A—Mathematical Physical and Engineering Sciences* 454 (1998) 903–995.
[22] H.N. Ozguven, D.R. Houser, Dynamic analysis of high speed gears by using loaded static transmission error, *Journal of Sound and Vibration* 125 (1) (1998) 71–83.
[23] H.N. Ozguven, A non linear mathematical model for dynamic analysis of spur gears including shaft and bearing dynamics, *Journal of Sound and Vibration* 145 (2) (1991) 239–260.
[24] W. Bartelmus, Mathematical modelling and computer simulation as an aid to gearbox diagnostics, *Mechanical Systems and Signal Processing* 15 (5) (2001) 855–871.
[25] D.C.H. Yang, Z.S. Sun, A rotary model for spur gear dynamics, *ASME Journal of Mechanical Transmissions and Automation in Design* 107 (1985) 529–535.
[26] J.H. Kuang, Y.T. Yang, An estimate of mesh stiffness and load sharing ratio of a spur gear pair, *Proceedings of the ASME 12th International Power Transmission and Gearing Conference*, Scottsdale, AZ, DE-43, 1992, pp. 1–10.